Open Access
ChemistryOPEN
Full Papers

POxylated Dendrimer-Based Nano-in-Micro Dry Powder Formulations for Inhalation Chemotherapy

Rita B. Restani,[a] Rita F. Pires,[b] Anna Tolmatcheva,[c] Rita Cabral,[c] Pedro V. Baptista,[c] Alexandra R. Fernandes,[c] Teresa Casimiro,[a] Vasco D. B. Bonifácio,*[b] and Ana Aguiar-Ricardo*[a]

Dedicated to Prof. Martyn Poliakoff on the occasion of his 70th birthday

POxylated polyurea dendrimer ($PURE_{G4}OOx_{48}$)-based nanoparticles were loaded with paclitaxel (PTX) and doxorubicin (DOX) and micronized with chitosan (CHT) by using supercritical CO_2-assisted spray drying (SASD). Respirable, biocompatible, and biodegradable dry powder formulations (DPFs) were produced to effectively transport and deliver the chemotherapeutics with a controlled rate to the deep lung. In vitro studies performed with the use of the lung adenocarcinoma cell line showed that $DOX@PURE_{G4}OOx_{48}$ nanoparticles were much more cytotoxic than the free drug. Additionally, the DPFs did not show higher cytotoxicity than the respective nanoparticles, and DOX-DPFs showed a higher chemotherapeutic effect than PTX formulations in adenocarcinoma cells.

1. Introduction

Lung cancer is one of the most aggressive and severe diseases, and it causes millions of deaths worldwide.[1–3] The use of chemotherapeutics in cancer treatment is limited due to the poor solubility of the chemotherapeutics and high systemic toxicity, which lead to severe side effects.[4–6] To overcome these problems, one of the major strategies envisages the engineering of polymers that "smartly" carry the drug and release it in the tumor microenvironment by using a trigger (e.g. acidic pH, ≈ 6.7–6.9 or hyperthermia, ≈ 40–42 °C) without compromising its activity.[7–10] However, to attempt specific and reliable lung delivery, the design of the carrier is fundamental. Microspheres occupy a central focus for this purpose, as they can achieve appropriate morphological and aerodynamic properties.[11] For suitable pulmonary administration, an aerodynamic size in the range of 1 to 5 µm is known to be mandatory.[12]

This work is specifically focused on a pulmonary drug-delivery system able to enhance the therapeutic performance of two widely used drugs in the treatment of non-small-cell lung cancer, namely, paclitaxel (PTX) and doxorubicin (DOX).[13, 14] Phase I/II clinical trials in which inhaled DOX is used to treat lung cancer have already been performed.[15–17] Chitosan (CHT) is a natural polymer that can be easily processed by supercritical CO_2-assisted spray drying (SASD) to produce respirable and swellable microparticles,[18, 19] and the incorporation of POxylated polyurea dendrimer drug nanocarriers in their core was recently reported by us.[20] We also demonstrated that polyurea dendrimer nanoparticles POxylated using hydrophilic oligo-oxazolines triggered a 100-fold reduction in the median inhibitory concentration (IC_{50}) value of PTX relative to what was found in the free drug. This strategy was extended to the chemotherapeutic nano-in-micro dry powder formulations (DPFs) designed in this work.[21] The synergies between nano- and microparticles ensure a quick delivery to the lung and enhance drug accumulation in neoplastic cells, which allow for: a faster response to the drug, a reduction in drug dosage, and consequently, a decrease in the number of undesired side effects. Moreover, dry powder formulations offer the advantage of storing the drug in a dry state, which can confer long-term stability and sterility.

[a] Dr. R. B. Restani, Dr. T. Casimiro, Prof. Dr. A. Aguiar-Ricardo
LAQV, REQUIMTE, Departamento de Química
Faculdade de Ciências e Tecnologia
Universidade Nova de Lisboa
2829-516 Caparica (Portugal)
E-mail: air@fct.unl.pt

[b] R. F. Pires, Dr. V. D. B. Bonifácio
CQFM/IN and IBB—Institute for Bioengineering and Biosciences
Instituto Superior Técnico, Universidade de Lisboa
1049-001 Lisboa (Portugal)
E-mail: vasco.bonifacio@tecnico.ulisboa.pt

[c] A. Tolmatcheva, Dr. R. Cabral, Prof. Dr. P. V. Baptista, Dr. A. R. Fernandes
UCBIO, REQUIMTE, Departamento de Ciências da Vida
Faculdade de Ciências e Tecnologia, Universidade Nova de Lisboa
2829-516 Caparica (Portugal)

2. Results and Discussion

The effect of POxylated polyurea dendrimers ($PURE_{G4}OOx_{48}$) on the release profiles and toxicity of PTX and DOX was fully investigated to optimize the therapeutic efficacy of the nano-in-micro drug-delivery systems. The therapeutic potential of the nanoparticles was also evaluated by taking into consideration the solubility, which is a critical parameter for plasma half-life enhancement. FTIR spectroscopy and NMR spectroscopy were performed to understand the nature of the dendrimer–drug interactions. The FTIR spectra did not show a significant shift in the bands for the free and encapsulated drugs (see Supporting Information, Figure S1). The ^1H NMR spectra of encapsulated DOX showed a shift in the aromatic protons (see Figure S2).

With the goal of having a fully green process, the chemotherapeutic drugs were impregnated in the nanosystems by supercritical (sc) CO_2-assisted impregnation, but low loadings were achieved [(12.8 ± 0.5) and (4.90 ± 0.01) μg of PTX and (276 ± 2) and (275.0 ± 0.1) μg of DOX per 100 mg of $PURE_{G4}OEtOx_{48}$ and $PURE_{G4}OMeOx_{48}$, respectively]. Nevertheless, higher loadings could possibly be achieved by classic (solution-based) methods (not investigated in the present work). After drug encapsulation, respirable dry powders were produced in moderate to good yields by SASD (see Table 1).

The morphological and physicochemical properties and in vitro aerosolizable performance were determined to evaluate the stability of the particles and the lung-deposition profiles. The studied nano-in-micro formulations were obtained as amorphous powders [see the X-ray diffraction (XRD) patterns in Figure S3], organized in agglomerates (Figure 1) with narrow diameter sizes (1.6 to 2.2 μm, see Table 1).

Upon using these values and the determined CHT powder density (0.9 ± 0.1) g cm^{-3}, the aerodynamic diameter (d_{aer}) was estimated for each powder containing PTX (1.56 and 1.55 μm) or DOX (1.55 and 2.04 μm) for micronized dendrimers grafted with oligo(2-methyl-2-oxazoline) (OMeOx) and oligo(2-ethyl-2-oxazoline) (OEtOx), respectively (see Table 1). These aerodynamic diameters are considered, accordingly to the literature, within the required range to achieve deep lung deposition.[12]

The powder deposition of the aerosolized particles into different regions of the human respiratory system was estimated by using an Andersen cascade impactor (ACI). The method requires aerosolization of the powder formulations (three batches) contained in capsules through the same inhaler. High percentage emitted doses (EDs) were found, and values between
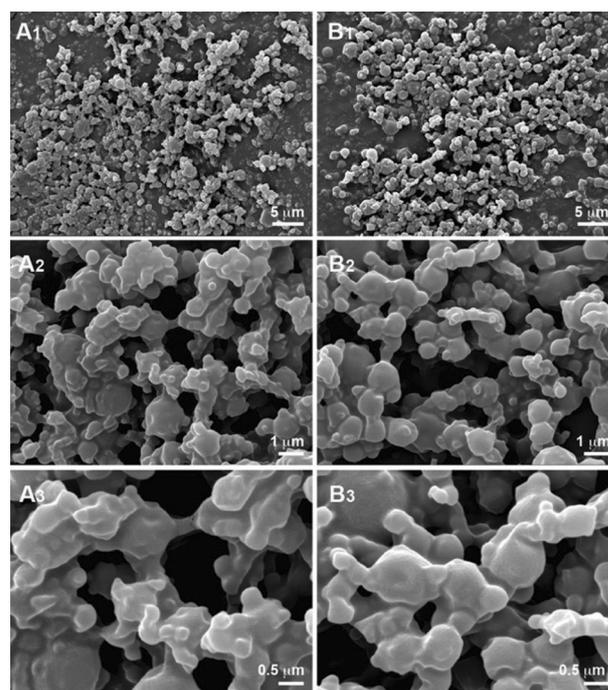

Figure 1. SEM images of A₁) $PURE_{G4}OMeOx_{48}[CHT]$ and B₁) $PURE_{G4}OEtOx_{48}[CHT]$ microparticles processed by supercritical-assisted atomization; the images in panels A₂/A₃ and B₂/B₃ are the corresponding magnifications.

(99.1 ± 0.3) and (99.6 ± 0.4)% revealed the ability of the powders to be aerosolized.

Further, the fraction of particles that could reach the alveoli (deep lung) was estimated through the fine particle fraction (FPF). The obtained values (> 28%) match those of most dry powder inhaler systems currently available on the market.[11] Only $PURE_{G4}OMeOx_{48}[CHT]$ loaded with PXT showed roughly 28% deposition; however, this is an independent value that can differ with the dispersion conditions. The average mass median aerodynamic diameter (MMAD) varied between (1.52 ± 0.01) and (3.10 ± 0.03) μm, and the geometric standard deviations (GSDs) ranged from 3.06 ± 0.01 to 3.84 ± 0.04 (Table 1).

The weight fraction according to the size distribution of the aerosolized particles is represented in Figure 2. As shown, although a high percentage of the dispersed formulations stay in the inhaler and in the induction port, a representative fraction is deposited in the deep lung.

Table 1. Characterization of nano-in-micro dry powder formulations.[a]

DPF	Yield [%]	$d_{v,50}$ [μm]	Span	Shape	Surface	T [°C]	H [%]	ED [%]	MMAD [μm]	FPF [%]	GSD	FPM [%]
PTX@$PURE_{G4}OMeOx_{48}[CHT]$	63	1.7	2.4	spherical	smooth	24.8	29	99.6 ± 0.4	1.52 ± 0.01	28 ± 2	3.82 ± 0.08	27.9
PTX@$PURE_{G4}OEtOx_{48}[CHT]$	75	1.7	2.3	spherical	smooth	24.8	29	99.1 ± 0.3	3.10 ± 0.03	31.4 ± 0.3	3.11 ± 0.02	31.7
DOX@$PURE_{G4}OMeOx_{48}[CHT]$	76	1.6	1.8	spherical	smooth	25.3	28	99 ± 2	1.61 ± 0.02	45 ± 1	3.84 ± 0.04	45.6
DOX@$PURE_{G4}OEtx_{48}[CHT]$	83	2.2	1.7	spherical	smooth	26.7	21	99 ± 4	1.58 ± 0.02	32 ± 1	3.06 ± 0.01	34.4

[a] H: humidity, ED: emitted dose, MMAD: mass median aerodynamic diameter, FPF: fine particle fraction, GSD: geometric standard deviation, FPM: fine particle mass.
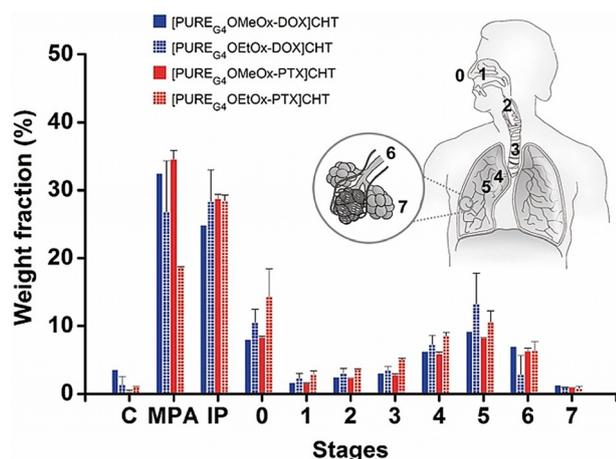
Figure 2. Comparison of the powder dispersion among different SADS processed powders loaded with DOX (blue bars) and PTX (red bars) by an eight-stage Andersen cascade impactor (ACI). Each bar represents the average of three repeats, and error bars refer to standard deviation. The picture shows the correspondence between the ACI stages and lung regions. C = capsule, MPA = mouthpiece adaptor, IP = induction port.
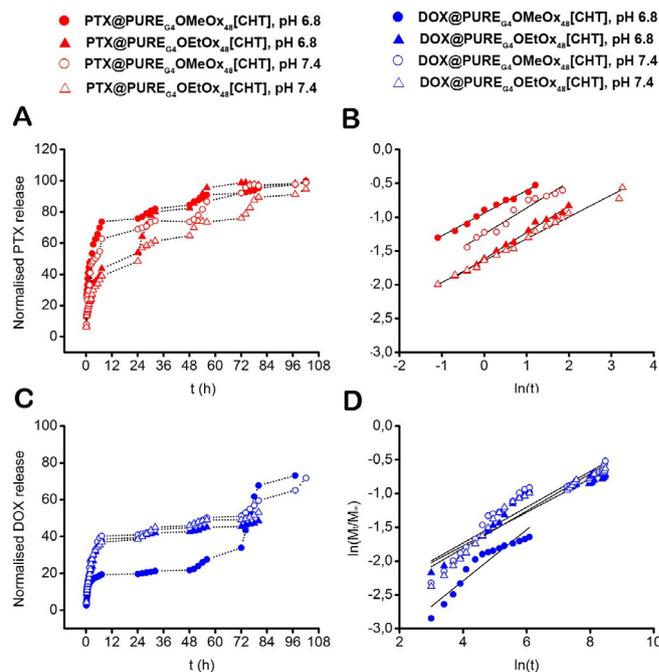

Figure 3. Release profiles of A) PTX and C) DOX and B, D) the corresponding release profiles fitted through the Korsmeyer–Peppas and Peppas–Sahlin mathematical models from the different nano-in-microparticles at pH 7.4 and 6.8 at 37 °C.

Literature reports in which dendrimer-based (and related systems using nano or nano-in-microparticles) inhalation dry powders are used are very scarce. For PTX delivery to the lungs, we did not find any study in which dendrimers were used. However, surfactant-based dry powder formulations show MMAD values (1.5–3.1 μm) that are similar to the MMAD values obtained for our system (1.9–2.3 μm). In this case, the FPFs reached stages three and four very efficiently (up to 87%).[22] Our PTX and DOX formulations reached stage five with an acceptable FPF (up to 31%). Regarding DOX formulations, polyethylene glycol (PEG)ylated poly(amidoamine) (PAMAM)–DOX conjugates, a dendrimer-based system, was reported to show adequate MMAD values (1.2–3.3 μm) and a high FPF (up to 78%), reaching stage five.[23]

The drug-release profiles were evaluated at pH values that mimic the environment of the lungs (pH 7.4) and the extracellular matrix of the tumor (pH 6.8) at 37 °C and at an ionic strength of 10 mm (Figure 3). The drug concentration was set below the saturation concentration documented for PTX, which presents low solubility in aqueous solution (0.3 μg mL^{-1}). As seen from Figure 3, $PURE_{G4}OMeOx_{48}$ showed more sustained DOX release than the other matrices: rapid release up to only 20% in the first 6 h, mild release until 72 h, and again fast release up to 70% until 96 h. The other matrices showed faster DOX release in the first 6 h, up to 40%, and then mild and controlled release up to 80 h. In the case of PTX release, it was faster from $PURE_{G4}OMeOx_{48}$ (pH 6.8) up to around 75% in the first 10 h, and then it became smooth and controlled up to almost 100% until 108 h. The other matrices showed the same trend but with decreasing rates in the following order: OMeOx (pH 7.4) > OEtOx (pH 6.8) > OEtOx (pH 7.4).

The fitting of data up to 60% drug release in the cumulative curves was performed by using the Korsmeyer–Peppas and the Peppas–Sahlin mathematical models (Figure 3). The Fickian diffusion coefficient (n) was determined for all formulations and

was higher than 0.2 in all cases (Table 2). Considering the diffusion constant (k_d) and the relaxation constant (k_r), the release mechanism was found to be primarily due to relaxation phenomena, especially for pH 7.4, and this is characteristic of non-Fickian release transport.

Viability studies were initially performed in the A549 adenocarcinoma cell line by using the MTS [3-(4,5-dimethylthiazol-2-yl)-5-(3-carboxymethoxyphenyl)-2-(4-sulfophenyl)-2H-tetrazolium] assay, as represented in Figure 4. Cytotoxicity studies were undertaken by keeping the concentration of each drug constant within each system to evaluate the formulations' performance relative to that of the free drugs.

The viability assay was undertaken considering the relative IC$_{50}$ determined after incubation of the A549 adenocarcinoma cell line with increasing concentrations of DOX and PTX for a 48 h period (Figure 4 a, b and Table S1). The data in Figure 4 reveal that depending on the drug loaded into the nanoparticle a different response is observed.

$PURE_{G4}OMeOx_{48}$ loaded with DOX was more cytotoxic in the A549 cell line than $PURE_{G4}OMeOx_{48}$ loaded with PTX. In fact, $PURE_{G4}OMeOx_{48}$ was the most effective carrier, as it induced higher cytotoxicity than $PURE_{G4}OEtOx_{48}$ (for PTX) or the free drug (for DOX). One possible explanation for this behavior are the different hydrophobic characters of both oligomers. As OMeOx is less hydrophobic, drugs tend to escape faster from this matrix compared to formulations containing the PURE dendrimer grafted with OEtOx. Indeed, this agrees with the results observed in Figure 3.

Additionally, the observed variability in the viability results may be explained on the basis of the sizes, charge, macromo-

Table 2. Constants obtained through the fitting of the drugs release profiles by using the Korsmeyer–Peppas and Peppas–Sahlin mathematical models.[a]

Microparticle	pH	Korsmeyer–Peppas			Peppas–Sahlin			
		R^2	k	n	R^2	k_d	k_r	m
PTX@PURE$_{G4}$OEtOx$_{48}$[CHT]	7.4	0.9899	0.1983	0.3226	0.9875	0.0102	0.0599	0.1530
	6.8	0.9554	0.2872	0.3845	0.9786	0.0586	0.0499	0.1601
PTX@PURE$_{G4}$OMeOx$_{48}$[CHT]	7.4	0.9870	0.3909	0.3359	0.9896	0.0909	0.1038	0.1156
	6.8	0.9930	0.1934	0.3906	0.9902	0.0252	0.0202	0.2170
DOX@PURE$_{G4}$OEtOx$_{48}$[CHT]	7.4	0.9178	0.0546	0.2751	0.9885	0.0005	0.0860	0.2115
	6.8	0.9056	0.0614	0.2649	n.a.	n.a.	n.a.	n.a.
DOX@PURE$_{G4}$OMeOx$_{48}$[CHT]	7.4	0.9195	0.0629	0.2483	0.9956	0.0034	0.1432	0.1002
	6.8	0.9029	0.0222	0.3870	n.a.	n.a.	n.a.	n.a.

[a] R^2: correlation coefficient, k: kinetic constant, n: diffusion exponent, k_d: diffusion constant, k_r: relaxation constant, m: purely Fickian diffusion exponent, n.a.: not applicable.
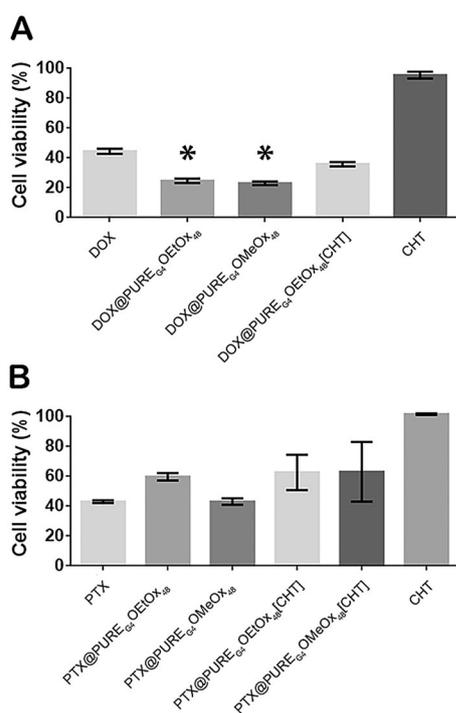

Figure 4. Cytotoxicity of the formulations and the free drugs in the A549 adenocarcinoma cell line. A549 cells were treated for 48 h with the relative IC$_{50}$ of each drug: A) 9.2 μm DOX and B) 0.1 μm PTX, and cell viability was determined by the MTS assay. The data were normalized against the control treated with 0.1 % (v/v) DMSO. The results shown are expressed as mean ± SEM of three independent assays. The symbol * indicates that the results are statistically significant with $p < 0.05$ (as compared to the free drug—DOX or PTX).

lecules assembling, and nature of the surface groups that are available to interact with the cells' membrane.[24] Given that different cytotoxic effects were observed in adenocarcinoma cells, additional cytotoxicity studies were performed in a colorectal carcinoma cell line model with the aim to provide further extension of these formulations to other cancer models and in healthy human cells to understand further their potential side effects in normal cells. In this regard, the HCT116 colorectal carcinoma cell line, healthy human mammary epithelial cells, and healthy human primary fibroblasts were separately exposed to the PTX and DOX formulations for 48 h, and cell via-

bility was then assessed. Interestingly, in agreement with the adenocarcinoma cell line results (Figure 4), the PURE$_{G4}$OMeOx$_{48}$ nanoparticles (loaded with PTX in this case) showed the highest cytotoxicity in the colorectal carcinoma cell model (Figure S4). These results are extremely interesting and should be further explored, as no effect on cell viability was observed for any of the nanoparticles in healthy cell lines (Figure S5).

Evaluating the nano-in-microparticles in terms of cytotoxicity, no further improvements, for the tested period, were observed compared to the effect of the free drugs or nanoformulations; nevertheless, the DOX-loaded nano-in-microparticles showed a higher effect than the PTX-loaded nano-in-microparticles in adenocarcinoma cells (see Figures 4 and S4). The fact that the cytotoxicity of the nano-in-microparticles is lower than that of the nanoparticles might be due to slower drug release during the testing period, as swelling and erosion of the matrix can affect release. Therefore, these carriers should be tested for longer periods of incubation in adenocarcinoma cells, and in vivo studies should also be performed, as different results can be attained in a much more complex environment.

3. Conclusions

Engineered nano-in-microparticles were formulated with two common anticancer drugs, doxorubicin and paclitaxel. These POxylated dendrimer-based formulations were investigated to understand their performance and potential in inhalation chemotherapy. Chitosan-based biodegradable microparticles, produced by supercritical CO$_2$-assisted spray drying, showed proper flowability properties for inhalation delivery, including an acceptable mass median aerodynamic diameter and a narrow distribution size. Toxicity assays performed with the A549 and HTC116 cell lines revealed that the microparticles prepared with nanoparticles having a polyurea core and a less hydrophobic oligooxazoline shell (OMeOx) were the most suitable. These preliminary results are highly promising, but additional studies are required to understand fully the release mechanism and way of action.

Experimental Section

Materials and Methods

Paclitaxel was kindly provided by Xi'an Rongsheng Biotechnology Co., Ltd. Doxorubicin hydrochloride was supplied from Apollo Scientific Ltd. Carbon dioxide UN1013 was obtained from Air Liquid. The POxylated polyurea dendrimers ($PURE_{G4}OMeOx_{48}$ and $PURE_{G4}OEtOx_{48}$) were synthesized as reported.[18] FTIR spectra were obtained with a PerkinElmer Spectrum 1000 instrument. Samples were cast directly onto NaCl disks, and the dry powder formulations were analyzed by using KBr pellets (1% *w/w* of powder in KBr) with a resolution of 1 cm^{-1} and 16 scans. NMR spectra were recorded with a Bruker ARX 400 MHz equipment. The morphology of the particles was accessed by scanning electron microscopy (SEM). Samples were mounted on aluminum stubs by using carbon cement (D-400, Neubaeur Chemikalien) and were gold coated. The images were obtained with a Hitachi S-2400 instrument with an accelerating voltage of 15 kV. The particle size was determined by a particle analyzer system (Morphologi G3 Essentials, from Malvern Instruments Ltd). More than 30000 particles were considered in each particle-size distribution calculation. Span, which represents the width of the particle distribution, was calculated by using Equation (1):

$$\text{Span} = \frac{d_{V;\,90} - d_{V;\,10}}{d_{V;\,50}} \qquad (1)$$

in which $d_{V,90}$, $d_{V,50}$, and $d_{V,10}$ are the particle diameters in volumes corresponding to 90, 50, and 10% of the population, respectively. The X-ray diffraction (XRD) patterns were obtained by treating the samples in a RIGAKU X-ray diffractometer, model Miniflex II. Samples were placed in a holder and were analyzed through CuKα radiation (30 KV/15 mA), with a 2θ angle ranging from 2 to 55° and a scan rate of 1°min^{-1}.

Synthesis

Encapsulation of Paclitaxel (PTX) and Doxorubicin (DOX) into POxylated Polyurea Dendrimers

A 33 mL stainless-steel high-pressure cell was equipped with a metallic net as a physical barrier between the drug and the polymers. Briefly, $PURE_{G4}OEtOx_{48}$ or $PURE_{G4}OMeOx_{48}$ (400 mg) was placed on top of the net, and the bottom of the cell was charged with PTX (20 mg) and a magnetic stirrer. The reactor was closed with two aligned sapphire windows and was connected to a CO_2 high-pressure line, charged with CO_2 to approximately 0.1 MPa, and placed in a thermostatted water bath at 40 °C. Subsequently, the pressure was adjusted to 25 MPa by the addition of more CO_2 to solubilize the drug. After 20 h, rapid depressurization of the cell was performed. The DOX loading was performed following the same protocol but by using a pressure of 22 MPa and 12 mg of the drug.

PTX: FTIR (NaCl film): $\tilde{v} = 1734, 1704, 1646, 1242, 1177, 1096$ cm^{-1}.

PTX@$PURE_{G4}OEtOx_{48}$: FTIR (NaCl film): $\tilde{v}$ 1734, 1620, 1421, 1191, 1055 cm^{-1}.

PTX@$PURE_{G4}OMeOx_{48}$: FTIR (NaCl film): $\tilde{v} = 1738, 1615, 1415, 1241, 1034$ cm^{-1}.

DOX: ^{1}H NMR (400 MHz, D_2O): $\delta = 7.59$ (m), 7.33 (m), 5.39 (br s), 4.17 (m), 3.83 (s), 3.76 (s), 3.62 (m), 2.91 (br s), 2.86 (br s), 2.58 (br s), 2.53 (br s), 2.18 (m), 1.95 (m), 1.24 ppm (d).

DOX@$PURE_{G4}OEtOx_{48}$: ^{1}H NMR (400 MHz, D_2O): $\delta = 8.13$ (br s), 8.07 (br s), 7.94 (br s), 3.53 (m), 2.42–2.31 (m), 1.07 ppm (m).

DOX@$PURE_{G4}OMeOx_{48}$: ^{1}H NMR (400 MHz, D_2O): $\delta = 8.07$ (br s), 8.03 (br s), 7.94 (br s), 3.55 (m), 2.11 ppm (m). The signals for doxorubicin, with the exception of the aromatic region, are masked by the signals of the dendrimer.

PTX Quantification in POxylated Polyurea Dendrimers

Samples were washed with water (3 mL) by stirring for 4 h, filtered with a 0.1 μm Millipore filter, and dried under vacuum. Next, the sample (70 mg) was placed overnight in the dark with chloroform (4 mL) with strong stirring to release the drug from the dendrimers. To remove the dendrimer, the mixture was washed with water (2×3 mL), and the chloroform phase was dried under vacuum. The drug content was determined in triplicate by HPLC (Knauer) by using a C18 column (250 mm L×4.6 mm inner diameter) with 5 μm particles. A mixture of acetonitrile and water (60:40) was used as the mobile phase, delivered at 0.6 mL min^{-1}. The column effluent was detected at $\lambda = 230$ nm with a UV detector. The column temperature was maintained at 25 °C, and the injected volume was 20 μL. The calibration curve for PTX quantification was performed in the range of standard concentration of PTX at 0.2–17 μg mL^{-1} with a good correlation coefficient ($R^2 = 0.99996$).

DOX Quantification in POxylated Polyurea Dendrimers

Samples were washed with methanol (3 mL) by stirring for 4 h, filtered with a 0.1 μm Millipore filter, and dried under vacuum. Next, the sample (100 mg) was placed overnight in the dark with acetonitrile (4 mL) with strong stirring to release the drug from the dendrimers. To remove the dendrimer, the mixture was filtered with a 0.1 μm Millipore filter, and acetonitrile was removed under vacuum. The drug content was determined in triplicate by HPLC with a Dionex apparatus by using a Interchim column (150 mm L× 4.6 mm inner diameter) with 5 μm silica gel particles. A mixture of acetonitrile and 50 mm sodium acetate at pH 4 (70:30) was used as the mobile phase at a flow rate of 0.6 mL min^{-1}. The column effluent was detected at $\lambda = 254$ nm with a UV detector. The column temperature was maintained at 25 °C, and the injected volume was 20 μL. The calibration curve for DOX quantification was performed in the range of standard concentration of 25–300 μg mL^{-1} with a good correlation coefficient ($R^2 = 0.99994$).

Production of Nano-in-Micro Dry Powder Formulations

Chitosan (CHT, 2.5 g) was dissolved in 1% aqueous acetic acid with stirring for 24 h. The solution was filtered and drug@$PURE_{G4}OEtOx_{48}$ or drug@$PURE_{G4}OMeOx_{48}$ (360 mg) dissolved in ethanol (14.5 mL) was added. The mixture was homogenized by stirring and was fed to a laboratory-scale SASD apparatus. After liquefying in a cryogenic bath, liquid CO_2 was pumped through a high-pressure HPLC pump (K-501, Knauer) into a heated bath and was then mixed and solubilized within the polymeric liquid solution in the static mixer pressurized through a high-pressure HPLC pump (305 Gilson). The static mixer promoted mixing of scCO$_2$ and the liquid solution at near-equilibrium conditions. A static mixer 3/16, model 37-03-075 from Chemieer was used (internal diameter 4.8 mm and length

191 mm, with 27 helical mixing elements). The homogenized solution was then sprayed out, at atmospheric pressure, through a nozzle (inner diameter 150 μm) into the precipitator, which was equipped with two sapphire windows on opposite sides to allow visualization of the spraying process. Temperature control was performed by a set of heating tapes that covered its external surface and were connected to an Isopad TD 2000 heat controller ($\pm 0.1\,°C$ stability). The pressure into the precipitator was measured by using a Setra pressure indicator (± 0.1 psi stability). The temperature of the static mixer was controlled by a set of heating tapes connected to a LDS temperature controller. A flow rate of heated compressed air was delivered into the precipitator to assist rapid liquid solvent evaporation from the particles. At the end of the precipitator, a cyclone enabled separation of the atomized particles from the flow stream, the gases were discharged by ventilation, and the powder was collected at the bottom of the cyclone in a suitable container. SASD co-precipitation produced spherical microparticles in an amorphous solid state, in which the drug was entrapped and homogeneously dispersed ($pCO_2 = 10$ MPa; $T_{mix} = 80\,°C$; $T_{precip} = 90\,°C$).

Powder Dispersion and Sizing by Cascade Impaction

The dispersibility of the dry powders was assessed by using an aluminum Andersen cascade impactor (ACI) apparatus (Copley). The powder was dispersed at a steady flow rate of about 60 L min^{-1}. An inhaler was attached to the inlet of the ACI that was fixed on the testing stand horizontally. The flow rate was maintained by a high-capacity pump model HCP5 (Copley) through the sampling apparatus to simulate inhalation. Five capsules n°3 (Aerovaus) containing about 30 mg of the formulations were individually loaded into the inlet of the Aerolizer Plastique 60LPM—Model 7 dry powder inhaler (DPI). The eight metal plates within the impactor were coated with filters (Glass Microfibre Filters, MFV1 diameter 80 mm, Filter Lab). Before assembling the apparatus, the inhaler and all filters were weighed on an analytical balance. The air flow was regulated in a critical flow controller model TPK (Copley) until a pressure drop of 4 kPa was achieved, and the flow of air was measured by using a flowmeter model DFM3 (Copley); the time for each run was then determined by applying Equation (2):

$$t\ [\mathrm{s}] = \frac{4L}{Q_{air}} \times 60 \qquad (2)$$

in which Q_{air} [L min^{-1}] is the air flow measured with the flowmeter and $4L$ is the inhaled air sample volume required by Cascade Impaction measurements. Critical flow must be guaranteed by maintaining the ratio between the pressures upstream and downstream of the flow control valve (pressures $P_3/P_2 \leq 0.5$).[25] Then, each capsule was released from an Aerolizer inhaler under the tested conditions for the determined time, as reported in the European Pharmacopeia.[26] After dispersion, the inhaler and all the filters were weighed again. For accuracy, each test was repeated three times. The emitted dose (ED) corresponds to the total loaded powder exiting the capsule and was calculated by using Equation (3):

$$\mathrm{ED}\ [\%] = \frac{m_{full} - m_{empty}}{m_{powder}} \times 100 \qquad (3)$$

in which m_{full} [mg] and m_{empty} [mg] are the weights of the capsule before and after simulating the inhalation, and m_{powder} [mg] is the initial weight of the powder introduced in the capsule. The capsules were prepared in the same way and with the same weight as previously determined for the Shot Weight protocol of the European Pharmacopeia.[27] The fine particle fraction (FPF) was determined by interpolation of the percentage of the particles containing less than 5 μm. The mass median aerodynamic diameter (MMAD) was determined as the particle diameter corresponding to 50% of the cumulative distribution. The geometric standard deviation (GSD) was determined by using Equation (4):

$$\mathrm{GSD} = \sqrt{\frac{d_{84}}{d_{16}}} \qquad (4)$$

in which d_{84} and d_{16} are the diameters corresponding to 84 and 16% of the cumulative distribution, respectively.

Biological Methods

In Vitro PTX Release Profile

The impregnated microparticles (≈ 150 mg) were suspended in citrate-phosphate buffer solution (10 mL, pH 7.4 and 6.8) with ionic strength of 10 mm at 37 °C and aliquots (1 mL) were withdrawn periodically; the same volume of fresh medium was added to the suspension. The samples were lyophilized and 1.5% methanol in dichloromethane (1 mL) was added to the tubes. The amount of drug present in each sample was quantified by UV/Vis spectroscopy at $\lambda = 290$ nm by external standard calibration. The corresponding drug-release profiles were represented through plots of percent PTX cumulative release (calculated from the total amount of PTX contained in each matrix) versus time. The total mass of released drug in each moment of the experiment was calculated by taking into account the aliquots taken and the dilution factor by the addition of fresh buffer.

In Vitro pH-Triggered DOX Controlled Release

The impregnated microparticles (≈ 50 mg) were suspended in citrate-phosphate buffer solution (10 mL, pH 7.4 and 6.8) at 37 °C and aliquots (1 mL) were withdrawn periodically; the same volume of fresh medium was added to the suspension. The amount of DOX present in each sample was quantified by UV/Vis spectroscopy at $\lambda = 487$ nm by external standard calibration. The corresponding drug-release profiles were represented through plots of percent DOX cumulative release (calculated from the total amount of DOX contained in each matrix) versus time. The total mass of drug released in each moment of the experiment was calculated by taking into account the aliquots taken and the dilution factor by the addition of fresh buffer. The total drug encapsulation into the microparticles was determined by milling a fixed amount of co-atomized powders. The solution was stirred for 2 h and was then centrifuged at 15000 rpm for 5 min. The supernatant was then collected, and the amount of drug was determined by UV/Vis spectroscopy at $\lambda = 487$ nm.

Modeling of the Drug Release

The drug release was modeled for the first 60% of release by using the Korsmeyer–Peppas[28] and Peppas–Sahlin[29] mathematical models.

Cell Culture

Human colorectal carcinoma (HCT116) and lung adenocarcinoma (A549) cells were grown in Dulbecco's modified Eagle's medium (DMEM) (Invitrogen Corp., Grand Island, NY, USA) supplemented with 10% fetal bovine serum and 1% antibiotic/antimycotic solution (Invitrogen Corp.) and were maintained at 37°C in a humidified atmosphere of 5% CO_2 as previously described.[30,31] Healthy human fibroblasts were grown under similar conditions, supplemented with 1% minimum essential medium (MEM) nonessential amino acid (Invitrogen Corp.). The MCF10A cell line was cultured in the same medium as healthy human fibroblasts supplemented with 100 ng mL^{-1} cholera toxin (Lonza/Clonetics Corporation). All cell lines were purchase from ATCC (www.atcc.org).

Formulations and Drug Exposure

Stock solutions containing the formulations were prepared in sterile double-distilled water. For the dose–response curves, cells were plated at 5000 cells per well in 96-well plates. Media were removed 24 h after plating and were replaced with fresh media containing: each formulation containing 0.42 μm DOX and 7.5 nm PTX for the HTC116 cell line and 9.2 μm DOX and 0.1 μm PTX for the A549 cell line, CHT, or water (vehicle controls).

Viability Assays

After 48 h of cell incubation in the presence or absence of each compound, cell viability was evaluated with a CellTiter 96 AQueous Non-Radioactive Cell Proliferation Assay (Promega, Madison, WI, USA) by using 3-(4,5-dimethylthiazol-2-yl)-5-(3-carboxymethoxy-phenyl)-2-(4-sulfophenyl)-2H-tetrazolium, inner salt (MTS). In brief, this is a homogeneous, colorimetric method to determine the number of viable cells in proliferation, cytotoxicity, or chemosensitivity assays. The conversion of MTS into the aqueous soluble formazan product is accomplished by dehydrogenase enzymes found in metabolic active cells. The quantity of the formazan product was measured in a Bio-Rad microplate reader Model 680 (Bio-Rad, Hercules, CA, USA) at $\lambda = 490$ nm, as absorbance is directly proportional to the number of viable cells in culture.

Statistical Analysis

All data are expressed as mean ± SEM from at least three independent experiments. Statistical significance was evaluated by using the Student's t-test; $p < 0.05$ was considered statistically significant.

Acknowledgements

Conflict of Interest

The authors declare no conflict of interest.

[1] J. Ferlay, D. M. Parkin, E. Steliarova-Foucher, *Eur. J. Cancer* **2010**, *46*, 765–781.

[2] A. Jemal, R. Siegel, E. Ward, Y. Hao, J. Xu, M. J. Thun, *CA Cancer J. Clin.* **2009**, *59*, 225–249.

[3] D. R. Youlden, S. M. Cramb, P. D. Baade, *J. Thorac. Oncol.* **2008**, *3*, 819–831.

[4] C. E. Ashley, E. C. Carnes, G. K. Phillips, D. Padilla, P. N. Durfee, P. A. Brown, T. N. Hanna, J. Liu, B. Phillips, M. B. Carter, N. J. Carroll, X. Jiang, D. R. Dunphy, C. L. Willman, D. N. Petsev, D. G. Evans, A. N. Parikh, B. Chackerian, W. Wharton, D. S. Peabody, J. Brinker, *Nat. Mater.* **2011**, *10*, 389–397.

[5] A. Babu, A. K. Templeton, A. Munshi, R. Ramesh, *J. Nanomater.* **2013**, *2013*, 1–11.

[6] Z. Zhang, L. Mei, S. S. Feng, *Expert Opin. Drug Delivery* **2013**, *10*, 325–340.

[7] J. Shi, P. W. Kantoff, R. Wooster, O. C. Farokhzad, *Nat. Rev. Cancer* **2017**, *17*, 20–37.

[8] M. Karimi, A. Ghasemi, P. S. Zangabad, R. Rahighi, S. M. M. Basri, H. Mirshekari, M. Amiri, Z. S. Pishabad, A. Aslani, M. Bozorgomid, D. Ghosh, A. Beyzavi, A. Vaseghi, A. R. Aref, L. Haghani, S. Bahrami, M. R. Hamblin, *Chem. Soc. Rev.* **2016**, *45*, 1457–1501.

[9] H. M. Abdelaziz, M. Gaber, M. M. Abd-Elwakil, M. T. Mabrouk, M. M. El-gohary, N. M. Kamel, D. M. Kabary, M. S. Freag, M. W. Samaha, S. M. Mortada, K. A. Elkhodairy, J. Y. Fang, A. O. Elzoghby, *J. Controlled Release* **2018**, *269*, 374–392.

[10] E. Ayano, M. Karaki, T. Ishihara, H. Kanazawa, T. Okano, *Colloids Surf. B* **2012**, *99*, 67–73.

[11] I. M. El-Sherbiny, H. D. C. Smyth, *Mol. Pharm.* **2012**, *9*, 269–280.

[12] B. Y. Shekunov, P. Chattopadhyay, H. H. Y. Tong, A. H. L. Chow, *Pharm. Res.* **2007**, *24*, 203–227.

[13] D. H. Johnson, J. H. Schiller, P. A. Bunn Jr, *J. Clin. Oncol.* **2014**, *32*, 973–982.

[14] S. Ramalingam, C. P. Belani, *Expert Opin. Pharmacother.* **2004**, *5*, 1771–1780.

[15] Memorial Sloan Kettering Cancer Center and National Cancer Institute, *Inhaled Doxorubicin in Treating Patients with Primary Lung Cancer or Lung Metastases*, Clinical trial NCT00004930, completed in February, **2004**.

[16] G. A. Otterson, M. A. Villalona-Calero, S. Sharma, M. G. Kris, A. Imondi, M. Gerber, D. A. White, M. J. Ratain, J. H. Schiller, A. Sandler, M. Kraut, S. Mani, J. R. Murren, *Clin. Cancer Res.* **2007**, *13*, 1246–1252.

[17] G. A. Otterson, M. A. Villalona-Calero, W. Hicks, X. Pan, J. A. Ellerton, S. N. Gettinger, J. R. Murren, *Clin. Cancer Res.* **2010**, *16*, 2466–2473.

[18] R. P. Cabral, A. M. L. Sousa, A. S. Silva, A. I. Paninho, M. Temtem, E. Costa, T. Casimiro, A. Aguiar-Ricardo, *J. Supercrit. Fluids* **2016**, *116*, 26–35.

[19] A. Aguiar-Ricardo, *Curr. Opin. Green Sustainable Chem.* **2017**, *5*, 12–16.

[20] R. B. Restani, A. S. Silva, R. F. Pires, R. Cabral, I. J. Correia, T. Casimiro, V. D. B. Bonifácio, A. Aguiar-Ricardo, *Part. Part. Syst. Charact.* **2016**, *33*, 851–858.

[21] R. B. Restani, J. Conde, R. F. Pires, P. Martins, A. R. Fernandes, P. V. Baptista, V. D. B. Bonifácio, A. Aguiar-Ricardo, *Macromol. Biosci.* **2015**, *15*, 1045–1051.

[22] S. A. Meenach, K. W. Anderson, J. Z. Hilt, R. C. McGarry, H. M. Mansour, *AAPS PharmSciTech* **2014**, *15*, 1574–1587.

[23] Q. Zhong, S. R. P. da Rocha, *Mol. Pharm.* **2016**, *13*, 1058–1072.

[24] A. Panariti, G. Miserocchi, I. Rivolta, *Nanotechnol. Sci. Appl.* **2012**, *5*, 87–100.

[25] M. Bonam, D. Christopher, D. Cipolla, B. Donovan, D. Goodwin, S. Holmes, S. Lyapustina, J. Mitchell, S. Nichols, G. Pettersson, C. Quale, N. Rao, D. Singh, T. Tougas, M. Van Oort, B. Walther, B. Wyka, *AAPS PharmSciTech* **2008**, *9*, 404–413.

[26] Council of Europe in *Eur. Pharmacopeia 5.1*, **2004**, 2843–2847.

[27] Council of Europe in *Eur. Pharmacopeia 7.0*, **2010**, 274–285.

[28] P. L. Ritger, N. A. Peppas, *J. Controlled Release* **1987**, *5*, 23–36.

[29] N. A. Peppas, J. J. Sahlin, *Int. J. Pharm.* **1989**, *57*, 169–172.

[30] O. A. Lenis-Rojas, A. R. Fernandes, C. Roma-Rodrigues, P. V. Baptista, F. Marques, D. Pérez-Fernández, J. Guerra-Varela, L. Sánchez, D. Vázquez-García, M. López Torres, A. Fernández, J. J. Fernández, *Dalton Trans.* **2016**, *45*, 19127–19140.

[31] A. S. Mendo, S. Figueiredo, C. Roma-Rodrigues, P. A. Videira, Z. Ma, M. Diniz, M. Larguinho, P. M. Costa, J. C. Lima, A. J. Pombeiro, P. V. Baptista, A. R. Fernandes, *J. Biol. Inorg. Chem.* **2015**, *20*, 935–948.

www.chemistryopen.org